SECOND EUROPEAN CONFERENCE ON EARTHQUAKE ENGINEERING
AND SEISMOLOGY, ISTANBUL AUG. 25-29, 2014

# DEVELOPMENT OF LIFE-TIME SEISMIC FRAGILITY CURVES FOR AGING BRIDGES

Behrouz SHAFEI[1] and Alice ALIPOUR[2]

## ABSTRACT

Reinforced concrete (RC) highway bridges are subjected to deteriorating mechanisms during their life-cycle. These mechanisms have adverse effects on the durability of bridges and can potentially make them vulnerable in terms of serviceability and ultimate limit states. Corrosion-induced deterioration can be identified in several forms, such as mass and strength loss of rebars, cracking and spalling of the concrete cover, and loss of bond between the concrete and steel. The structural degradation must be evaluated on a regular basis to determine the available structural capacity and schedule the required preventive actions. The current paper studies the extent and likelihood of deterioration of RC bridges located in chloride contaminated environments and investigates the effects of chloride-induced corrosion on the life time performance of these bridges. In this study, the corrosion initiation time is calculated through a detailed computational model considering the most influential parameters, including ambient temperature, relative humidity, chloride binding capacity, and exposure conditions. Also a detailed mechanical model is provided to consider the effect of corrosion on decreasing the cross sectional area of steel, yield strength of steel and the loss of the concrete cover.

## INTRODUCTION

The Reinforced Concrete (RC) structures are exposed to many deteriorating processes during their service life time. The performance of such structures is highly dependent on the changing properties of concrete and steel reinforcement due to these deteriorating mechanisms. Therefore there is an urgent need to develop a reliable computational method which is capable of making reliable predictions of life-cycle performance of the bridges. The corrosion process consists of two major phases, initiation and propagation. To make reliable decisions an accurate estimation of time corresponding to each of these stages is required.

The durability of concrete structures is adversely affected by intrusion of aggressive chemical substances into concrete. The chemical intrusion into concrete itself barely influences the performance of the structure but the presence of such chemicals results in lowering the pH in concrete and depassivation of the protection film around the steel rebar, which in turn results in initiation of corrosion process. For the structures located in coastal regions and subjected to air-borne chloride or those located in cold regions with harsh winters and exposed to deicing salts, chloride-induced corrosion is a major cause of deterioration of the structural components.

Chloride induced corrosion takes place when the concentration of chloride ions in the pore solution in the vicinity of reinforcing bar reaches a threshold value, which is high enough to depassivate the protection film around the steel rebar. Chloride transport mechanism in concrete is a

[1] Assistant Professor, University of Massachusetts Amherst, shafei@engin.umass.edu
[2] Assistant Professor, University of Massachusetts Amherst, alipour@umass.edu

complex phenomenon which may occur in several forms (i.e., ionic diffusion, capillary suction, permeation, etc.) and is dependent on the characteristics of the concrete (i.e., pore size distribution, water to cement ratio, etc.), the degree of pore saturation, exposure conditions, chloride binding capacity, and free chloride content as well as the duration of time in which the structure has been exposed to such conditions. Depending on all these conditions the deterioration process of the reinforcing steel in RC structures may be relatively fast and result in cracking or spalling of the concrete with a detrimental effect on structural serviceability and safety.

In this paper the holistic model proposed by Shafei (2011) is used to simulate the corrosion initiation time. Then the remaining capacity of the structure after corrosion initiation is calculated. This is accomplished by application of the crack propagation model developed by Alipour (2010). Moreover models to relate the corrosion rate to the structural deterioration such as cracking and spalling of the concrete cover, reduction of steel bar cross section area, and reduction of bond strength between concrete and reinforcing bar are considered. Finally the life-time seismic performance of these structures is estimated using the concept of fragility analysis.

## MATHEMATICAL DEFINITION OF CHLORIDE INTRUSION

It is assumed that the dominant mode of chloride intrusion into concrete is diffusion. Diffusion is the motion of chloride ions within the pore solution in response to the ion concentration gradient. It is described by the Fick's first law and is based on mass conservation principal. The chloride ions concentrated on the exposed concrete surface diffuse into the cement matrix due to the ion concentration gradient. The diffusion of chloride ions into partially saturated concrete can be described using the following partial differential equation (Saetta et al., 1993):

$$J_{Cl} = -D_{Cl}\,\omega_e.\nabla\left(C_f\right) \tag{1}$$

where $J_{Cl}$ is the flux of the chloride ions in a unitary area in a unit of time, $D_{Cl}$ is the chloride diffusion coefficient/diffusivity, $\omega_e$ is the evaporable water content, $C_f$ is the free chloride concentration, and the negative sign indicates diffusion in the opposite direction of increasing chloride concentration. The equation of chloride mass conservation (i.e., Fick's second law) is (Saetta et al., 1993):

$$\frac{\partial C_t}{\partial t} = div(J_{Cl}) = -div\left[D_{Cl}\,\omega_e.\nabla\left(C_f\right)\right] \tag{2}$$

where $C_t$ is the total chloride concentration in the unitary volume of porous body and $t$ is time. The relationship between total, $C_t$, free, $C_f$, and bound, $C_b$, chloride content in unsaturated concrete is as following:

$$C_t = C_b + \omega_e C_f \tag{3}$$

Substituting Equation 3 in Equation 2, free chloride diffusion equation is obtained as:

$$\frac{\partial C_f}{\partial t} = -div\left[D_a \nabla\left(C_f\right)\right] \tag{4}$$

where $D_a$ is the apparent diffusion coefficient that is influenced by the adsorption phenomena.

$$D_a = \frac{D_{Cl}}{1+(1/\omega_e)\left(\partial C_b/\partial C_f\right)} = D_{Cl}.F_1(C_b) \tag{5}$$

where $\partial C_b/\partial C_f$ is the chloride binding capacity. Chloride binding capacity could be defined using three different binding isotherms; linear, Langmuir, and Freundlich. Figure 1 depicts the relationship between the free chloride content, binding capacity and $F_1(C_b)$. It could be understood from Figure 1 that all binding isotherms result in reduction of $F_1(C_b)$ and $D_a$ eventually. More details on the chloride binding capacity, evaporable water content, the binding isotherms, and their dependency on different parameters such as temperature, humidity, aging, and free chloride content could be found in Shafei et al. (2012 and 2013).

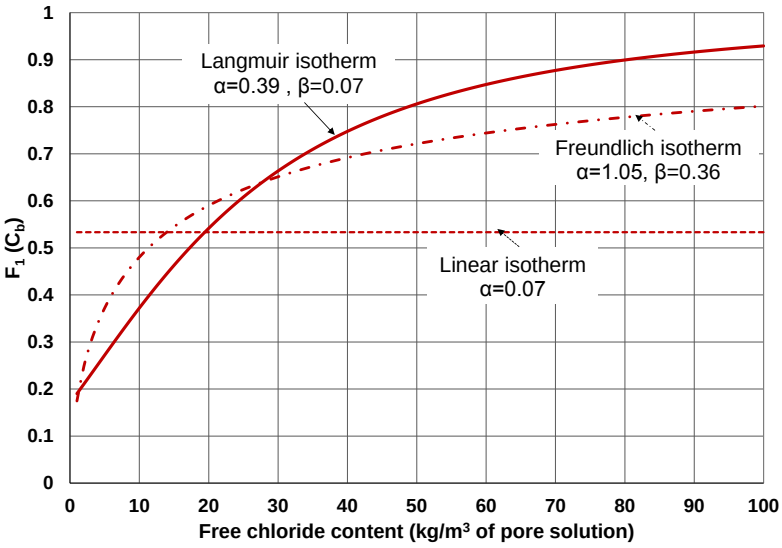


Figure 1. Effects of chloride binding capacity and free chloride content on $F_1(C_b)$

## NUMERICAL SOLUTION

The governing partial differential equation given by Equation 4 cannot be solved without using numerical methods because of dependence of $D_a$ on nonlinear, time-dependent parameters. Equation 4 is solved here as a boundary value problem in space and as an initial value problem in time by use of finite difference formulation. The reason to develop a numerical solution in this paper is to study the effect of different time-dependent, nonlinear parameters on the chloride intrusion procedure, to estimate the corrosion initiation time. The value for chloride content at time zero is considered to be zero indicating that no chlorides have been added to the concrete mixture. Using this finite difference method, a set of simultaneous equations were solved in time steps equal to one day, until the chloride profile in concrete depth at different time steps was calculated.

To start the analysis, the exposure condition (i.e., surface chloride content) of the RC member is required. Surface chloride content may depend on the composition of the concrete, position of the structure, orientation of its surface and microenvironment, chloride concentration in the environment and the general conditions of exposure with regard to rain and wind (Bertolini, 2008). In coastal regions, there are different types of exposure to chloride. Some structures (or some parts of them, i.e., piers) are submerged in the sea water. Some structures are located in tidal or splash zones and some other are just located in a close distance from the coast line, which makes them vulnerable to sea salt spray (water-borne chloride ions carried by the wind). It should be noted that the intrusion of chloride ions through an atmospheric condition (i.e., sea salt spray) happens in much lower rate compared to the tidal, splash, or submersion zones. A long term monitoring of surface chloride content on concrete structures shows the order of surface chloride with regard to the contact to sea water as following: tidal> splash> sea spray ( Uji et al., 1990). A full review of the studies collecting the data from different coastal conditions could be found in Alipour et al. (2013 a and b). In this paper we will only consider the sea salt spray exposure condition with a 5.0 kg/m$^3$ chloride surface content for a bridge located on the coast.

## CORROSION INITIATION TIME

Corrosion initiation time is determined as the time when the chloride concentration at the vicinity of reinforcing steel reaches the critical chloride concentration, i.e., $C_f(t_i, C) = C_{critical}$. Many studies in the literature have proposed values for the critical chloride content. Some conclude that since only free chlorides take part in corrosion process and those bounded to the hydrated cement have no effect, the chloride threshold content should be represented as the free chloride content. However the study by

Glass and Buenfeld (1999) on the chemical aspects of binding has shown that bound chloride may also affect the corrosion initiation, therefore the threshold value should be represented as the total chloride of content. There is also no agreement whether these chloride values (i.e., free or bound chloride content) should be shown relative to the weight of cement or concrete or as the chloride to hydroxyl concentration ratio, $Cl^-/OH^-$ (Glass and Buenfeld, 1997). The total critical chloride content for this study will be considered as 1% of cement weight (≈ 350 kg/m$^3$).

The total chloride content profiles are shown in Figure 2. The corrosion initiation time is evaluated by finding the intersection of chloride profile and the critical chloride content (=3.5 kg/m$^3$). In this example the concrete cover is assumed to be 50 mm, and applying the threshold chloride content the values for initiation time will be 9.33 years, 10.40 years and 12.66 years for linear, Freundlich and Langmuir isotherms, respectively. These values of corrosion initiation time are within the usually observed range of 7-20 years (Kong et al., 2002). It is evident that different chloride binding isotherms result in obvious changes of time of initiation, which indicates the importance of a reasonable choice for the binding model. In this paper the corrosion initiation time calculated using the Freundlich isotherm will be the basis of any further calculations.

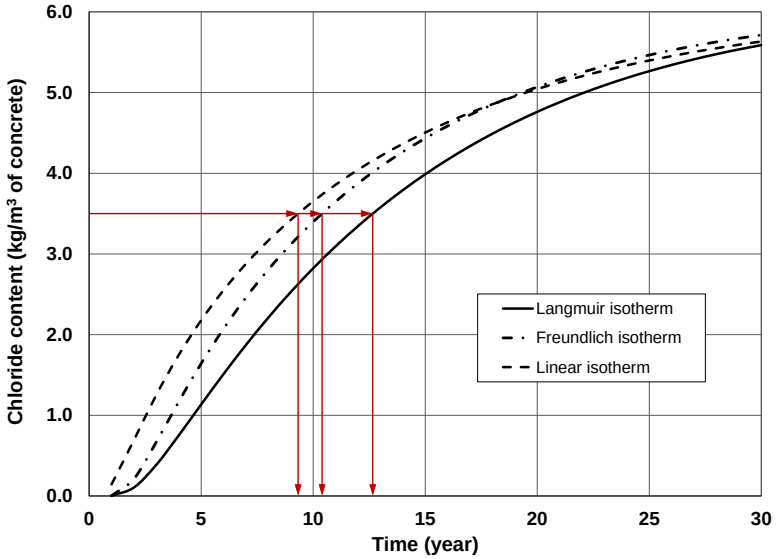


Figure 2. Estimation of corrosion initiation time using different binding isotherms

## CRACK INITIATION AND PROPAGATION

The concrete around the rebar is considered to be a thick-walled concrete cylinder of a homogeneous material (El Maadawy and Soudki 2007). The rust material produced during the corrosion process has a larger volume compared to that of steel used in the process. This causes an additional displacement in concrete, $\delta_c$. The relationship between radial pressure, $P_{corr}$, and concrete displacement is given by:

$$\delta_c = kP_{corr} \tag{6}$$

where $k$ is the concrete hole flexibility constant that relates the radial displacement to the internal pressure acting on the thick-walled concrete cylinder. Since there is a porous zone at the steel-to-concrete interface, the corrosion products must first fill this zone before their expansion starts to create pressure on the surrounding concrete. This porous zone will be included in the derivation of the concrete hole flexibility, $k$, from Equation 6 that can be found in standard text books on elasticity (e.g. Timoshenko):

$$\delta = \frac{a}{E_{eff}}\left[\frac{b^2+a^2}{b^2-a^2} + \upsilon\right]P \tag{7}$$

where $E_{eff}$ is concrete's effective elastic modulus, $a$ is the internal radius of the cylinder, $b$ is the exterior radius of the cylinder, and $v$ is concrete's Poisson's ratio (= 0.18). There is a porous zone at the steel to concrete interface which the corrosion products must first fill before their expansion starts

to create pressure on the surrounding concrete. Introducing $D_0'=D_0+2\delta_0$, where $D_0$ is the diameter of the steel reinforcing bar and $\delta_0$ is the thickness of the porous zone, $a = D_0'/2$ and $b = C+D_0'/2$ where $C$ is the wall thickness of the cylinder, Equation 7 can be rewritten as follows:

$$\delta = \frac{D_0'}{2E_{eff}}[\psi + 1 + \upsilon]P \tag{8}$$

where $\psi = D_0^{'2}/2C(C+D)$. Hence the whole flexibility, $k$, from Equation 6 is given by:

$$k = \frac{DD_0'}{2E_{eff}}[\psi + 1 + \upsilon] = \frac{(\psi+1+\upsilon)(D_0+2\delta_0)}{2E_{eff}} \tag{9}$$

The prediction of the internal radial pressure caused by corrosion requires a determination of thickness of rust, $\delta_r$, thickness of steel lost to form rust around the steel reinforcing bar, $\delta_l$, and thickness of the porous zone, $\delta_0$. $M_r$ denotes the mass of rust per unit length of one bar and $M_{loss}$ is the mass of steel per unit length consumed to produce, $M_r$. As shown in Figure 3, the formation of the rust layer results in increasing the bar diameter from $D_0$ to $D_0+2(\delta_r - \delta_l)$. Equating the increase in volume per unit length, calculated from the difference between volume of rust produced and volume of steel consumed per unit length, to the change in area expressed in terms of diameter change, gives:

$$\frac{M_r}{\rho_r} - \frac{M_{loss}}{\rho_s} = \pi D_0(\delta_0 + \delta_c) \tag{10}$$

where $\rho_r$ is the mass density of rust, $\rho_s$ is the mass density of the steel, and $D_0$ is the original diameter of the steel reinforcing bar.

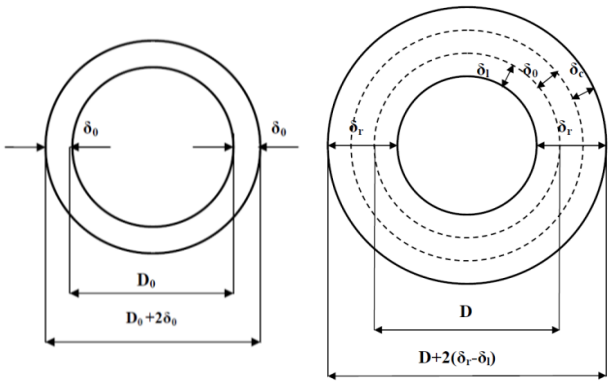


Figure 3. Change in reinforcing bar diameter due to corrosion

The relationship between $M_r$ and $M_{loss}$ can be expressed as follows:

$$M_{loss} = \alpha M_r \tag{11}$$

where $\alpha$ is the ratio of molecular mass of steel to molecular mass of rust. To determine the relationship between the percentage steel mass loss, $m_l$ (=$100M_{loss}/M_{st}$), and the internal pressure caused by corrosion, the ratio of mass density of rust, $\rho_r$, to mass density of the original steel, $\rho_s$, is needed. This relationship can be expressed as $\rho_r = \beta\rho s$. The relative ratio of volume of expansive corrosion products to the volume of iron consumed in the corrosion process is $\gamma$ (=$1/\alpha\beta$). The pressure caused by corrosion, $P_{corr}$, can be calculated by combining Equations 6, 10, and 11:

$$P_{corr} = \frac{2\frac{M_{loss}}{\rho_s}E_{eff}(\gamma-1)}{\pi D_0(\psi+1+\upsilon)(D_0+2\delta_0)} - \frac{2\delta_0 E_{eff}}{(\psi+1+\upsilon)(D_0+2\delta_0)} \tag{12}$$

Negative values of $P_{corr}$ in Equation 12 stands for the period in which rust fills the voids around the bar and are set equal to zero. In order to express the internal radial pressure caused by corrosion as a function of the percentage steel mass loss the following relationship is used:

$$\frac{M_{loss}}{\rho_s} = \frac{M_{loss}}{M_{st}}\frac{M_{st}}{\rho_s} = \frac{m_1 A_{s0}}{100} = \frac{m_1 \pi D_0^2}{400} \tag{13}$$

where $A_{s0}$ is the original cross-sectional area of the steel reinforcing bar. Combining Equations 12 and 13, the relationship between the percentage steel mass loss and the internal radial pressure caused by corrosion is given by:

$$P_{corr} = \frac{E_{eff}[m_1 D_0(\gamma-1)-400\delta_0]}{200(\psi+1+\upsilon)(D_0+2\delta_0)} \quad (14)$$

The concrete ring is assumed to crack when the tensile stresses in the circumferential direction at every part of the ring have reached the tensile strength of the concrete. The radial pressure required to cause cracking of concrete cover, $P_{cr}$, is with is given by:

$$P_{cr} = \frac{2Cf_{ct}}{D_0} \quad (15)$$

The governing equation at cracking can then be determined by equating $P_{corr}$ from Equation 14 to Equation 15. Then the percentage of steel mass loss, $m_1$, corresponding to cracking initiation can be formulated as follows:

$$m_1 = \frac{400}{D_0^2(\gamma-1)E_{eff}}\left[C\, f_{ct}(\psi+1+\upsilon)(D_0+2\delta_0) + D_0\delta_0 E_{eff}\right] \quad (16)$$

To calculate the time to corrosion crack initiation the Faraday's Law will be used (Alipour et al. 2010). The mass of iron $M_{loss}$ consumed over time is related to the amount of current, $A$, that flows through the electrochemical corrosion cell. The process is prescribed by Faraday's law as $dM_{loss}/dt = I_{corr}A/nF$, where $A$ is the atomic weight of the ion being dissolved (i.e., Fe= 55.85 gr), and Faraday's constant $F$= 96,500 ($A$.sec). Very little is known on the chemical composition of corrosion product, hence the valancy of reaction, $n$, is usually taken as 2. It follows that $dM_{loss}/dt = 2.893\text{x}10^{-4} I_{corr}$. Thus the consumed mass of steel per unit length of anodic bar subjected to corrosion for a time period Δt (seconds) will be:

$$\Delta M_{loss}(t) = \begin{cases} 2.893\times10^{-4}\pi D_0 \quad i_{corr}\Delta t & (t = t_{init}) \\ 2.893\times10^{-4}\pi D_{red}(t)\, i_{corr}\, \Delta t & (t > t_{init}) \end{cases} \quad (\frac{gr}{cm}) \quad (17)$$

The volume of corroded steel can also be calculated as:

$$\Delta V_{loss}(t) = \frac{\Delta M_{loss}}{\rho_s} = \begin{cases} 3.70897\times10^{-5}\pi D_0 \;\; i_{corr}\, \Delta t & (t = t_{init}) \\ 3.70897\times10^{-5}\pi D_{red}(t-1) i_{corr}\, \Delta t & (t > t_{init}) \end{cases} \quad (18)$$

It is assumed that before the corrosion initiation time no corrosion has happened in the steel bar. After the corrosion initiation time the consumed mass and volume of the corroded steel can be calculated from Equations 17 and 18 using the initial diameter of the rebar. Then this value will be used to calculate the reduction in rebar diameter, this procedure will continue recursively. The reduced rebar diameter after each step of corrosion is calculated as:

$$D_{red}(t) = \sqrt{D_0^2 - 4\Delta V_{loss}(t)/\pi} \quad (19)$$

To estimate the crack initiation time, the value of $M_{loss}$ will be calculated in each of the steps and divided by the initial steel mass. The time corresponding to $M_{loss}$ equating $m_1$ is marked as the time to crack initiation.

## RESIDUAL CAPACITY OF THE CORRODED REINFORCEMENT

The residual capacity of corroded reinforcing bars was investigated experimentally by Du et al. (2005 a and b). They conducted both accelerated and simulated corrosion tests on bare bars and bars embedded in concrete, to investigate the mechanism of the reduction of capacity of corroded reinforcement. They concluded that the residual strength of the bars decreases significantly with corrosion penetration. They showed that their test results are in reasonable agreement with other studies, some of which were obtained under natural corrosion conditions (i.e., Andrade et al. 1991, Lee et al. 1996, Morinaga 1996). Therefore the empirical equations proposed by Du et al. (2005) will be used to calculate the reduction in the strength of corroded reinforcement.

$$f_y(t) = \big(1 - 0.005\, m_1(t)\big) f_{y0} \tag{20}$$

where $f_y(t)$ is the yield strength of corroded reinforcement at each time step, $f_{y0}$ is the yield strength of non-corroded reinforcement, and $t$ is the time elapsed since corrosion initiation (years).

## CORROSION INITIAITON AND CRACK PROPAGATION

The corrosion in reinforcement is modeled using the Faraday's law (Equations 16-20). The time in which the concrete starts cracking is marked as the time where the steel loss equals to target steel loss level $m_1$, and is estimated to be 51 days (0.14 year). Bridge management systems consider a crack width of 0.3 mm as the limit for serviceability failure; for the conditions under study, the time in which the crack width exceeds 0.3 mm is equal to 117 days (0.32 year). Considering the time required for crack initiation with the time to corrosion initiation (10.40 years using Freundlich isotherm), it could be observed that the former is negligible compared to the latter one. The reduced rebar cross section and yield strength of the steel at different time intervals (Table 1) will be used for the capacity evaluation of the case-study bridge in this study.

Table 1. Updated rebar diameter and steel yield strength at 5 year intervals

| **Parameter** | **10.4** | **15.4** | **20.4** | **25.4** | **30.4** | **35.4** | **40.4** |
|---|---|---|---|---|---|---|---|
| **D (mm)** | 36 | 34.83 | 33.66 | 32.49 | 31.32 | 30.15 | 28.98 |
| **$m_1$(%)** | 0 | 6.39 | 12.57 | 18.54 | 24.30 | 29.85 | 35.19 |
| **(1-0.005)$m_1$ (%)** | 0 | 0.97 | 0.94 | 0.91 | 0.88 | 0.85 | 0.82 |

## LIFE TIME PROBABILISTIC ANALYSIS

The case study bridge is adopted from Alipour (2010). It is three-span reinforced concrete box-girder bridge with two interior bents and two circular columns in each bent. Each span of the bridge is 30 m and the deck width is designed for four traffic lanes and is equal t0 23 m. The total concrete cross section of deck is approximately 12 $m^2$. Both columns of each bent have the same diameter and height. The height and diameter of the columns is 1.7 m and 7.5 m, respectively. More details on the bridge geometry and the modeling procedure in OpenSees could be found in Alipour et al. (2011) and Shafei and Alipour (2012 and 2013).

In order to assess the seismic performance of the bridges, nonlinear time-history analysis will be conducted. A suite of 60 ground motions that consist of three sets of records corresponding to earthquakes with 2%, 10%, and 50% probability of occurrence in 50 years will be used for the analysis. To perform fragility analysis, the column curvature ductility is taken here as the primary damage measure. The curvature ductility is defined as the ratio of maximum column curvature recorded from a nonlinear time-history analysis to the column yield curvature obtained from moment-curvature analysis. Following the procedure given by Priestley et al. (1996), the curvature ductility values of all the bridge cases are calculated under the set of 60 ground motions and then compared with damage limit states. In this study, the damage limit states are assumed to equal the ductility of 1.0, 2.0, 4.0, and 7.0 for the slight, moderate, major, and complete damage states, respectively. The suggested values are in accordance with the limit states available in the literature for similar bridges (Hwang et al., 2000, Choi et al., 2004, and Yang et al., 2009).

Under a ground motion excitation with the peak ground acceleration of $PGA_i$ (here i = 1, ..., 60), a bridge sustains failure in a specific damage state if its ductility is larger than the ductility corresponding to that damage state. The parameters of each fragility curve (i.e., median, $c_k$ and log-standard deviation, $\zeta_k$) are estimated using the maximum likelihood procedure given in Shinozuka et al. (2000). For the $k$-th damage state ($k$ = 1, 2, 3, and 4), the fragility curve is developed following the formula below:

$$F_k(PGA_i|\zeta_k, c_k) = \Phi\left[\frac{\ln(PGA_i/c_k)}{\zeta_k}\right] \tag{22}$$

where $F_k$ is the probability of exceeding the damage state of $k$, and $\Phi[.]$ is the standard normal distribution function. For the log-standard deviation ($\zeta_k$), it is seen that different deviation values may result in intersecting the fragility curves of different damage states. To avoid any intersection, Shinozuka et al. (2000) suggest considering one common standard deviation value for all the damage states. In this study a value of 0.6 is selected as the identical log-standard deviation.

To evaluate the effects of chloride-induced corrosion on the life-time seismic performance of RC bridges, the fragility curves are generated for the life-time of the case-study bridge after corrosion initiation. 50 years after the corrosion initiation, the overall average of median values obtained for the four damage states drops by 34%. For further illustration, the time-dependent fragility curves of the bridge are depicted in Figure 4. It can be understood from this figure that for a specific PGA value, the probability of exceeding any damage state increases over the time due to the corrosion process.

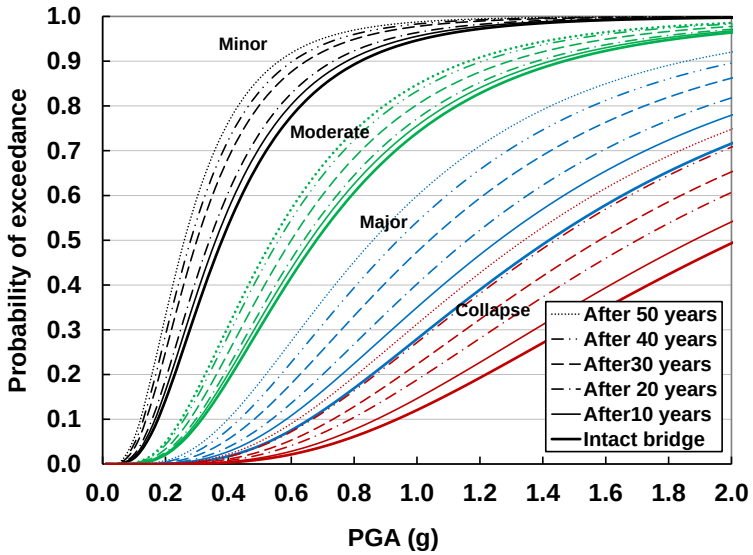


Figure 4. Life-time fragility curves for the three-span bridge with the medium span length and column height of 7.5 m

## CONCLUSIONS

This paper provides a framework that evaluates the life-cycle performance of deteriorating reinforced concrete highway bridges. The bridges under consideration are located in seismic areas and they are continuously exposed to the chloride ions attack. As a result, it is necessary to study the combined effects of a natural hazard and an environmental stressor over the time. Towards this goal, the current study first establishes a detailed computational approach which examines the chloride-induced corrosion by taking into account all the influential parameters. The simulation of chloride penetration into the concrete helps to obtain a more accurate estimate of the chloride content at different depths of reinforced concrete members and eventually a better prediction of the corrosion initiation time. The extent of structural degradation due to the corrosion process is also calculated to update the properties of structural members during the life-cycle of the bridge. Based on the characteristics of corroded bridges, the seismic response of a group of bridges with different structural attributes is evaluated and the level of performance reduction is quantified as a function of the elapsed time. The time-dependent seismic fragility curves of the bridges are then generated using a set of damage states for the purpose of seismic risk assessment.

**REFERENCES**


Alipour, A. (2010). *Life-cycle performance assessment of highway bridges under multi-hazard conditions and environmental stressors*. Ph.D. Dissertation, Department of Civil and Environmental Engineering, University of California, Irvine, CA.

Alipour, A., Shafei, B. and Shinozuka M. (2010). *Evaluation of uncertainties associated with design of highway bridges considering the effects of scouring and earthquake*. In: Proceedings of the 2010 Structures Congress, pp. 288-297.

Alipour, A., Shafei, B., and Shinozuka, M. (2011). *Performance evaluation of deteriorating highway bridges in high seismic areas*. ASCE Journal of Bridge Engineering, 16(5), pp. 597-611.

Alipour, A., Shafei, B. and Shinozuka M. (2013a). *Reliability-based calibration of load factors for LRF design of reinforced concrete bridge under multiple Eetreme events: scour and earthquake*. Journal of Bridge Engineering, 18(5), pp. 362-371.

Alipour, A., Shafei, B., and Shinozuka, M. (2013b). *Capacity loss evaluation of reinforced concrete bridges located in extreme chloride-laden environments*. Journal of Structure and Infrastructure Engineering, 9(1), pp. 8-27.

Andrade, C., Alonso, C., Garcia, D., and Rodriguez, J. (1991). *Remaining life time of reinforced concrete structures: effect of corrosion in mechanical properties of the steel, life prediction of corrodible structures*. In: Proceedings of the International Symposium of the National Association of Corrosion Engineers, Cambridge, U. K. p.12/1-12/11.

Ann, K. Y., Song, H. W., Lee, C. H., and Lee, K. C. (2006). *Build-up of surface chloride and its influence on corrosion initiation time of steel in concrete*. Structural Engineering and Construction, pp. 762-772

Bertolini, L. (2008). *Steel corrosion and service life of reinforced concrete structures*, Structure and Infrastructure Engineering, 4(2), pp. 123-137.

Choi, E., DesRoches, R., Nielson, B. (2004). *Seismic fragility of typical bridges in moderate seismic zones*. Journal of Engineering Structures, 26, pp. 187-199.

Du Y. G., Clark, L. A., and Chan, A. H. C. (2005a). *Residual capacity of corroded reinforcing bars*. Magazine of Concrete Research, 57(3), pp. 135-147.

Du Y. G., Clark, L. A., and Chan, A. H. C. (2005b). *Effect of corrosion on ductility of reinforcing bars*. Magazine of Concrete Research, 57(7), pp. 407-419.

El maaddawy, T., and Soudki, K. (2007). *A model for prediction of time from corrosion initiation to corrosion cracking*, Journal of Cement and Concrete Composites, 29, pp. 168-175.

Glass, G. K., and Buenfeld, N. R. (2000). *The influence of chloride binding on the chloride induced corrosion risk in reinforced concrete*. Corrosion Science, 42, pp. 329-344.

Hwang, H., Liu, J.B., Chiu, Y-H (2001). *Seismic fragility analysis of highway bridges*. Center of Earthquake Research and Information, University of Memphis.

Kong, J. S., Ababneh, A., N., Frangopol, D. M., and Xi, Y. (2002). *Reliability analysis of chloride penetration in saturated concrete*, Journal of Probabilistic Engineering Mechanics, 17 (3), pp. 302-315.

Lee, H.S., Tomosawa, F., and Noguchi, T. (1996). *Effect of rebar corrosion on the structural performance of single reinforced beams*. Durability of Building Material and Components, London, pp. 127-137.

Morinaga, S., (1996). *Remaining life of reinforced concrete structures after corrosion cracking*. Durability of Building Material and Components, London, pp. 127-137.

Saetta, A. V., Schrefler, B. A. and Vitaliani, R. V. (1993). *The carbonation of the concrete and the mechanism of moisture, heat and carbon dioxide flow through porous material*, Journal of Cement and Concrete Research, 23(4), pp. 761-772.

Shafei, B. (2011), *Stochastic finite-element analysis of reinforced concrete structures subjected to multiple environmental stressors*. Ph.D. dissertation, University of California, Irvine.

Shafei, B. and Alipour, A. (2012). *Vulnerability assessment of deteriorated bridges under seismic events*. In: Proceedings of the 15$^{th}$ World Conference on Earthquake Engineering (15WCEE), Lisbon, Portugal, September 24-28.

Shafei, B., Alipour, A., and Shinozuka, M. (2012). *Prediction of corrosion initiation in reinforced concrete members subjected to environmental stressors: A finite-element framework*. Journal of Cement and Concrete Research, 42(2), pp. 365-376.

Shafei, B. and Alipour, A. (2013). *Assessment of extent of capacity loss in deteriorated highway bridges*. In: Proceedings of the ASCE-SEI Structures Congress, Pittsburgh, PA, May 2-4.

Shafei, B., Alipour, A., and Shinozuka, M. (2013). *A stochastic computational framework to investigate the initial stage of corrosion in reinforced concrete superstructures*. Journal of Computer-Aided Civil and Infrastructure Engineering, 28(7), pp. 482-494.

Shinozuka, M., Feng, M.Q., Kim, H-K, Kim, S-H. (2000b). *Nonlinear static procedure for fragility curve development*. Journal of Engineering Mechanics, 126(12), pp.1287-1296.

Uji, K., Matsuoka, Y, and Maruya, T. (1990). *Formation of an equation for surface chloride content of concrete due to permeation of chloride*. Corrosion of Reinforcement in concrete. London, U. K., pp. 258-267.

Yang, C. S., DesRoches, R. and Padgett, J. E. (2009). *Fragility Curves for a Typical California Box Girder Bridge*. In: Proceedings of the 2009 ASCE Technical Council on Lifeline Earthquake Engineering Conference, San Francisco, CA, USA.